eISSN: 2976-1190

Journal of Engineering and Sciences

Vol. 4 Issue 1 May 30, 2025

DOI: 10.3126/jes2.v4i1.70746

Journal homepage: Journal of Engineering and Sciences (nepjol.info)

Publisher: Research Management Cell, Pashchimanchal Campus, Lamachour, Pokhara

Stability Analysis of a TBM Excavated Tunnel at a Critical Section between Main Boundary Thrust and Mahabharat Thrust using RS2 and RS3

Binod Bohara[1,2], Anish Aryal[2], Tek Bahadur Katuwal[1,3], Pursottam Shilpakar[4]

[1] *Department of Civil Engineering, IOE Pashchimanchal Campus, Tribhuvan University, Nepal*

[2] *TAC Hydro Consultancy Private Limited, Lalitpur, Nepal*

[3]*Norwegian University of Science and Technology (NTNU), Norway*

[4]*Jade Consult, Kathmandu, Nepal*

**Corresponding Author: beenodbohara@gmail.com*

(Manuscript Received: 08/10/2024; Revised: 14/12/2024; Accepted: 17/12/2024)

Abstract

This article demonstrates a detailed stability analysis of a tunnel excavated by a Tunnel Boring Machine (TBM) at a critical section between the Main Boundary Thrust (MBT) and Mahabharat Thrust (MT), a case study of Sunkoshi Marine Diversion Multipurpose Project (SMDMP) where double shield TBM was deployed to excavate the tunnel. The geological complexity in this area, including weak rock masses, poses severe challenges to TBM operations. We use the RS2 (2D) and RS3 (3D) numerical modeling software to assess the deformation, squeezing potential, and stress distribution at critical chainage, 4+669m. Rock mass classification based on the Rock Mass Rating (RMR) system was used to determine the quality of the surrounding rock and different empirical methods were applied to estimate rock mass strength and deformability. The results indicate significant deformation at chainage 4+669m, leading to TBM jamming as the installed thrust capacity of the machine was insufficient to overcome the shield friction.

Keywords: TBM; Deformation; Thrust Capacity; Shield Skin Friction.

1. Introduction

Tunneling in geologically complex regions, such as the Himalayan belt, poses significant engineering challenges due to the interaction between tectonic forces and variable rock mass conditions (KC et al., 2022).The Main Boundary Thrust (MBT) and Mahabharat Thrust (MT) are major tectonic features in the Himalayas, contributing to the terrain's geological complexity and instability.

Tunnels excavated by Tunnel Boring Machines (TBMs) in the Himalayan region are often subject to squeezing, deformation, and jamming, primarily due to high overburden pressures, poor rock mass quality, and tectonic stresses (Singh & Goal, 2006)This paper utilizes advanced numerical modeling techniques through RS2 (2D) and RS3 (3D) software to analyze the stability of the critical tunnel section. The model incorporates rock mass classification data, overburden depth, and in-situ stress conditions to simulate tunnel deformation and squeezing potential. Additionally, the required thrust to overcome the shield friction at the squeezed section is estimated based on Romani and Anagnostou's (2010) approach.

2. Methods and Methodology

2.1 Brief description of the project

The Sunkoshi Marin Diversion Multipurpose Project is located in the Sindhuli district, about 115 km southeast of Kathmandu. It is the second project in Nepal to use a Tunnel Boring Machine (Double Shield) for tunnel construction. The project serves two main purposes: (i)

diverting water from the Sunkoshi River, a surplus basin, to the Marin River, a tributary of the Bagmati River, and (ii) generating 31.07 MW of electricity. The project includes a 13.3 km long headrace tunnel with a diameter of 5.5 meters, designed to divert 67 cubic meters of water per second to the Marin River. This water will irrigate 122,000 hectares of agricultural land across the Bara, Rautahat, Sarlahi, Mahottari, and Dhanusha districts(Geotechnical Baseline Report of SMDMP, 2020). Geographically, the project lies between latitudes 27°20’38” N and 27°15’30” N and longitudes 85°59’03” E and 85°52’29” E. The area is seismically active, falling under a seismic hazard zone with a zoning factor (Z) of 0.4, according to NBC 105:2020.

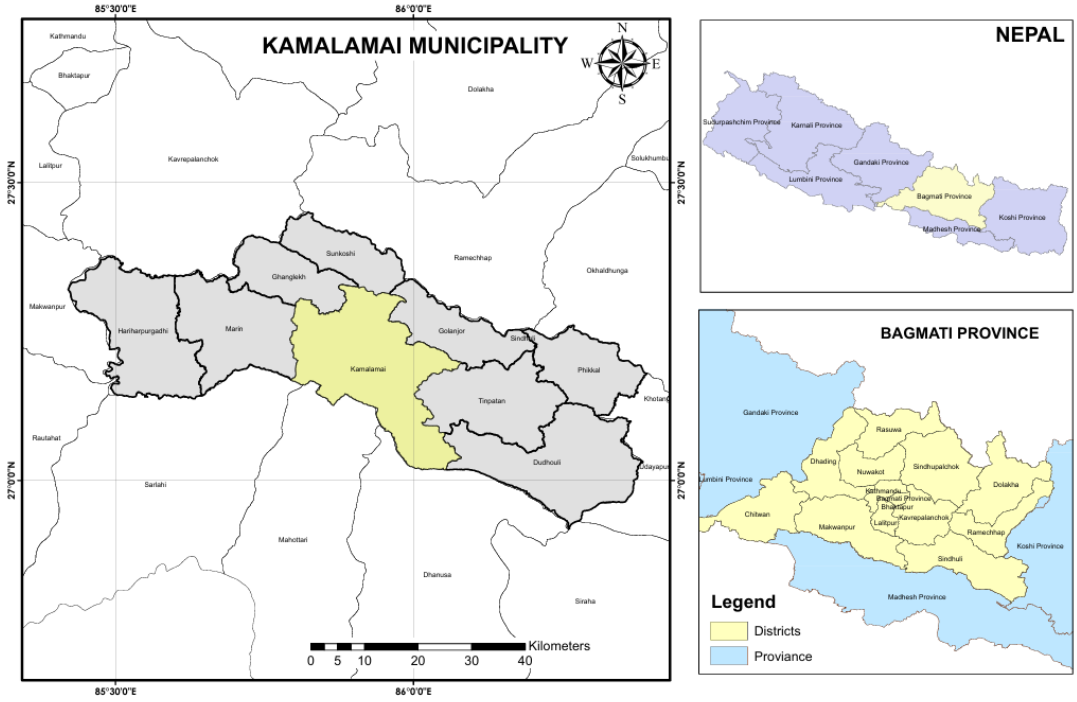

Figure 1: Location Map of Study Area

2.2 Geology of Project

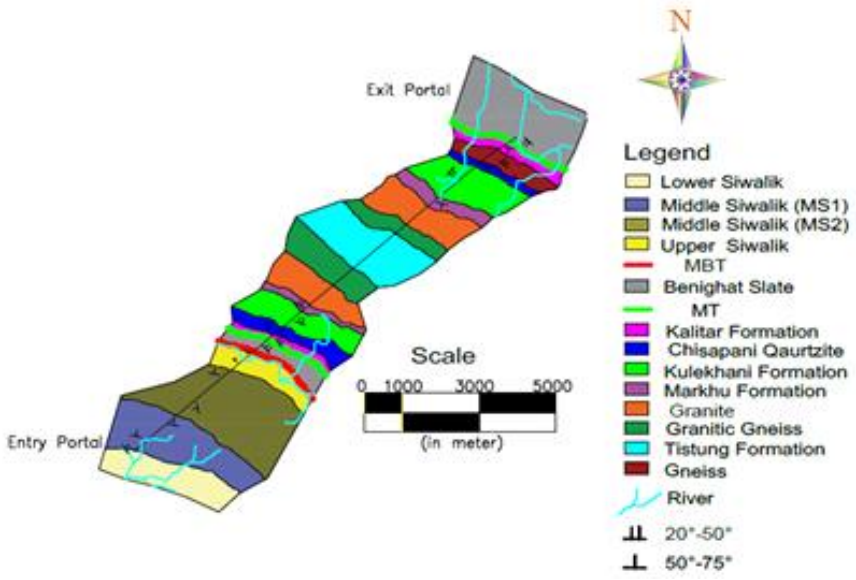

Figure 2: Geological map of SMDMP

The project area consists of rocks from the Siwalik Group and the Lesser Himalaya. The Siwalik Group contains sedimentary rocks, while the Lesser and Higher Himalayas have metamorphic and igneous rocks. The headrace tunnel crosses the Main Boundary Thrust (MBT) at one point and the Mahabharat Thrust (MT) at two locations. The first 4 km of the tunnel passes through Siwalik rocks, while the rest runs through a syncline structure with Higher Himalayan Gneiss and Granite at its core.

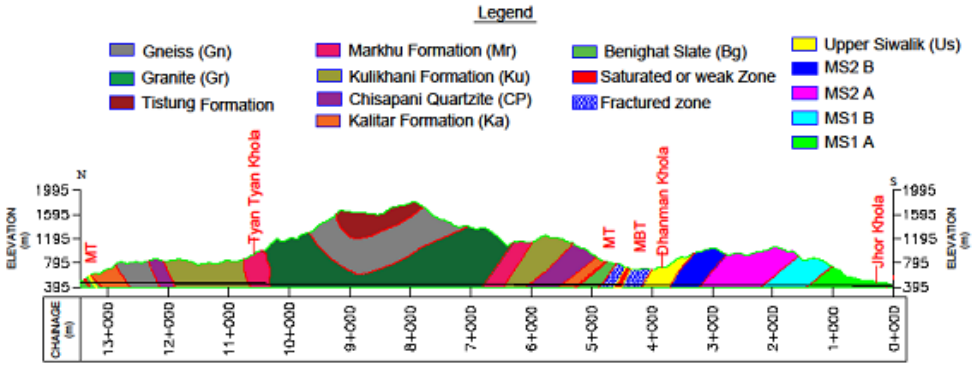

Figure 3: Geological cross-section of SMDMP

2.3 Geology of Critical Section

During the night shift on March 31, 2023, the TBM encountered unexpectedly weak geology consisting of low-strength phyllite with quartz veins at the face, contrary to prior predictions. The tunnel section between chainages 4+181m and 4+985m was initially expected to consist of fresh to moderately weathered, thin to medium bedded dolomite intercalated with thinly foliated slate and quartz veins(Geotechnical Baseline Report of SMDMP, 2020). Despite implementing various countermeasures, the TBM could not advance. The cutter head torque significantly increased, and both the forward and telescopic shields were squeezed, causing the TBM to halt at chainage 4+669m.

2.3.1 Geological Condition at TBM Stuck Location

The TBM became stuck in the Benighat Slate (Bg) geological section situated between the MBT and MT fault zones. The cross-section revealed phyllite with abundant quartz veins, mostly in a powdery form (80%), exhibiting poor self-stability and dry conditions. This suggests a high likelihood of extreme deformation, potential collapse, cutter head jamming, and shield squeezing. The geology encountered by various shields at the stuck position is detailed below.

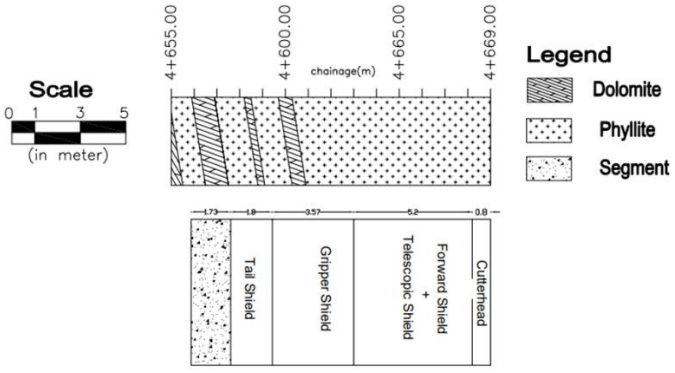

Figure 4: The position of TBM at stuck with respect to rock type it encountered (Bohara et al., 2023)

2.3.2 Cutter head, forward Shield, and telescopic Shield

The rock formation is entirely made up of phyllite (100%), characterized by very low strength. It contains a high concentration of quartz veins and lacks any underground water. This rock mass is classified as Category V, indicating that it is extremely unstable.

2.3.3 Gripper Shield and Tail Shield

The rock type observed consists of 90% phyllite and 10% dolomite. The phyllite contains quartz veins and is characterized by low strength (less than 5 MPa). The dolomite is moderately weathered and has medium to low strength, ranging from 5 to 15 MPa. The rock formation exhibits varying degrees of weathering and strength, primarily dominated by phyllite, followed by dolomite. The surrounding dolomite has a very short self-stabilizing time, while the phyllite section is extremely unstable.

2.4 Procedure for shield TBM stuck analysis

The research methodology begins with analyzing the section where the shield TBM (Tunnel Boring Machine) was stuck, followed by collecting geological details for the respective chainage. If the geological details indicate the presence of deformable rocks at the stuck section, it is concluded that the issue may be due to deformation. Deformation is then calculated using empirical methods and 2D and 3D numerical modeling. The calculated deformation is compared with the available overcutting space, which refers to the gap between the shield surface of the TBM and the excavated rock surface created by the cutter discs located at the circumference of the cutter head. If the deformation exceeds the maximum allowable overcutting space, the required thrust capacity is determined using nomograms (Ramoni & Anagnostou, 2010)The required thrust is then compared with the TBM's actual thrust capacity. The TBM is declared stuck if the machine’s thrust capacity is less than the required.

3. Result and Discussion

3.1 Mapped Rock Mass Quality

Table 1: Rock Mass Classification at the critical section

HRT Chainage [m]	Rock Type/ Rock Condition	RMR Value	Overburden H [m]
4+669	Weak Phyllite with quartz vein	16	350

Rock mass classification using the RMR system was conducted along the headrace tunnel from the manhole located at the bottom left of the cutter head. Parameters such as Uniaxial Compressive Strength (UCS), Rock Quality Designation (RQD), discontinuity spacing, discontinuity condition, and groundwater conditions were rated to classify the rock mass. The final RMR value was calculated by adding all parameters except for the orientation of discontinuities. Table 1 shows the rock mass observed at critical section 4+669m, which is rock class V with RMR value 16. The TBM got stuck at chainage 4+669m due to rock mass squeezing in both the forward and telescopic shields (Bohara et al., 2023).

3.2 Estimation of Rock mass parameters

The rock mass parameters along the headrace tunnel at the critical section have been calculated as shown in Table 2, which identifies various parameters like rock mass strength, s, a, and mb. The rock mass classification at the critical section is obtained in the form of RMR, which is converted to the GSI system. The value of the unit weight of rock and Poisson’s ratio were obtained from laboratory test results.

Table 2: Rock mass parameter along a critical section of headrace tunnel

HRT Chainage (m)	H (m)	σ_{ci} (MPa)	GSI	m_i	D	m_b	s	a	σ_{cm} (MPa)	E_{rm} (MPa)
4+669	350	34	11	7	0	0.29	0.00005	0.58	1.56	620.68

3.2.1 Rock Mass Strength

Rock mass strength is estimated using different empirical equations. Estimated rock mass strength with four empirical methods has been presented in Figure 5Hoek et al. (2002) and Barton (2002) give almost similar values for rock mass strength, whereas Kalamaras et al. (1995) give the lowest value, and Panthi (2006) give the highest value. Hoek et al. (2002) is considered relevant for our case since it is the approximate average of the other three methods.

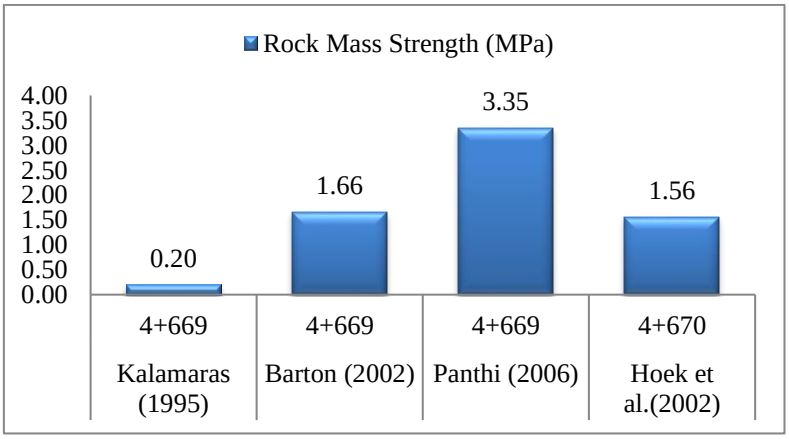

Figure 5: Rock mass strength using different empirical relations

3.2.2 Rock Mass Deformability

Rock mass deformability is also estimated using different empirical relations. Estimated rock mass strength with three empirical relations is presented in Figure 6. Panthi (2006) gives the highest value for rock mass deformability, whereas Hoek and Diederichs (2006) give the lowest value, and Hoek et al.'s (2002) value lies in the middle. So, Hoek et al. (2002) is considered relevant as it is the approximate average of the other two methods.

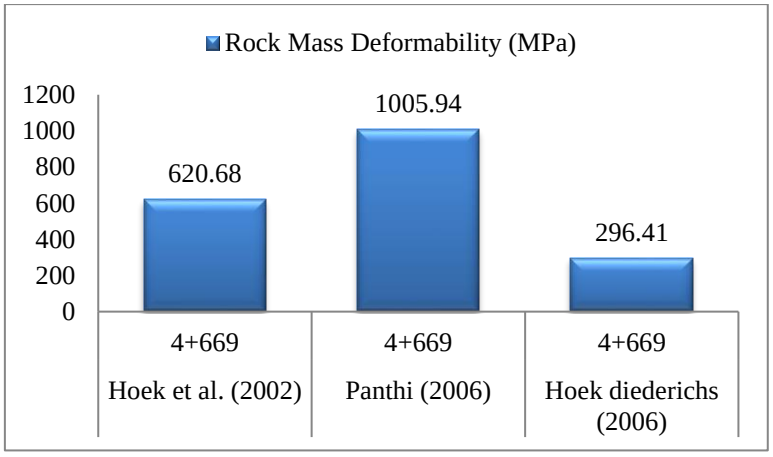

Figure 6: Rock mass deformability using empirical relations

3.3 Squeezing Assessment

3.3.1 Hoek and Marinos (2000) approach

It is a semi-analytical method that can predict the squeezing potential and measure its magnitude. It assumes a circular tunnel with a hydrostatic stress field where support pressure will act uniformly around the tunnel's periphery. At chainage, 4+669m, significant deformation of magnitude 472mm occurs, which is a very severe squeezing problem according to the categorization of Hoek and Marinos (2000). The deformation is more than void between the cutter head and shield even when maximum overcutting is done, i.e., 140 mm.

Table 3: Squeezing prediction by Hoek and Marinos (2000) approach

HRT Chainage	σ_{cm}/σ_v	Strain (∈ %) When Pi=0	Squeezing prediction	Deformation (mm) When Pi=0 MPa
4+669	0.165	7.38	Yes	472

3.3.2 Evaluation of Rock Stress

Overlying strata, tectonic movements, and topographic effects influence in-situ stress. Typically, these stresses are measured using methods like hydraulic fracturing and 3D over-coring(Hoek, 2007). However, since direct data for the site is unavailable, similar projects with comparable conditions were studied for reference.

The world stress Map shows that the approximate direction of tectonic stress for the Himalayas is almost parallel with the North-South direction, as shown in Figure 7. First of all, in-situ stress measurement data were searched within the radius of 50km of our project SMDMP with similar orientation and comparable characteristics, but no such data were found. So, the tectonic stress of 5MPa with orientation N10°E is assumed to be similar to the data used for many research works in Nepal. Still, to confirm, three-dimensional stress measurement is required and proposed as a suggestion. The in-situ stress is calculated due to gravity and tectonic stresses, which are summarized in Table 4.

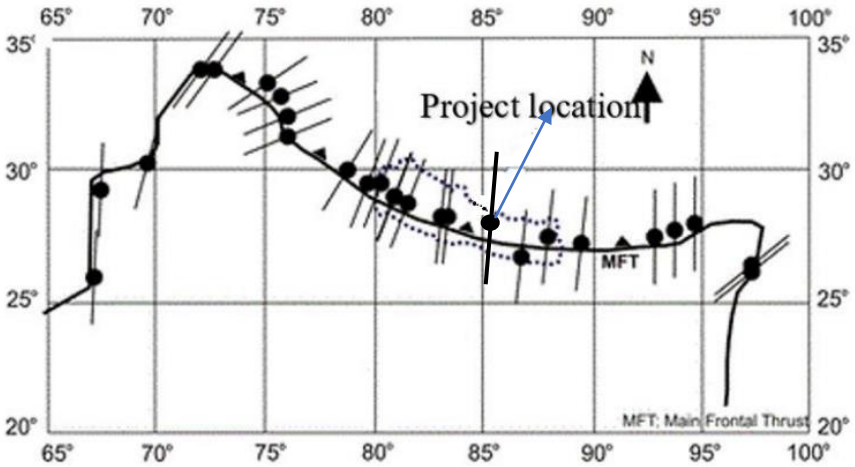

Figure 7: Approximate horizontal tectonic stress orientation based on World Stress Map. Note: stress tensors, and international boundary are not in true scale (Panthi, 2012).

3.3.3 Construction of Valley Model

To determine in-situ principal stresses, a 2D valley modeled representing a cross-section of a headrace tunnel using RS2 software as shown in Figure 8. The model has been set up as follows:

- The left and right sides are fixed horizontally (X direction).
- The top is free to move in both X and Y directions.
- The bottom far-end corners are constrained in both X and Y directions.
- Gravity-based field stress is applied, considering actual ground conditions.

The input parameter for the valley model is shown in Table 4.

Table 4: Input parameters for the valley model

Description	**Symbol**	**Unit**	**4+669m**
Overburden	H	m	350
Poisson's ratio	ν		0.31
Tectonic stress	σ_{tec}	MPa	5
The trend of tectonic stress	Θ_t	degree	N 10 °E
HRT trend	Θ_c	degree	N 50 °E
Density of rock	γ	MN/m^3	0.027
The angle between tectonic stress and HRT trend	α_t	degree	40
Vertical stress	σ_v	MPa	9.45
Horizontal stress due to gravity	σ_h	MPa	4.25
Total horizontal stress	σ_H	MPa	9.25
In-Plane horizontal stress	σ_α	MPa	7.179
Out-plane horizontal stress	$\sigma_{\alpha'}$	MPa	6.311
Locked in			
In-plane		MPa	2.934
Out of plane		MPa	2.066
Stress ratio			
In-plane			0.760
Out-Plane			0.668

After the modeling of the valley and its analysis, the value of major principal stress (σ_1), minor principal stress (σ_3), and intermediate principal stress (σ_z) were identified along with the stress direction angle (i.e., the angle made by σ_1 with horizontal) which is shown below in Table 5.

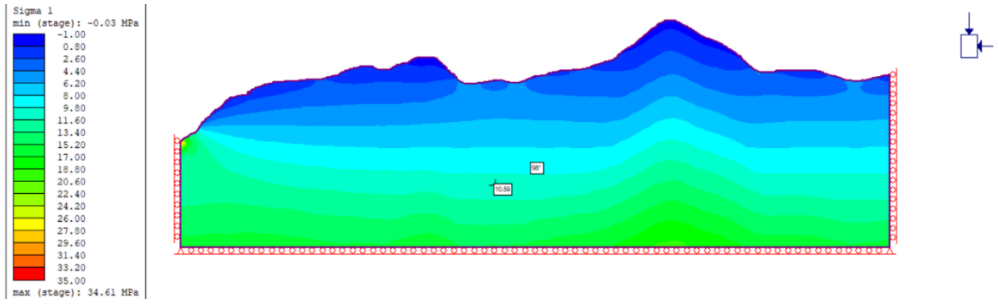

Figure 8: Valley model construction for headrace tunnel alignment at chainage 4+669m

Table 5: Output from valley model

Chainage (m)	**Valley Profile**			
	σ_1 (MPa)	**σ_3(MPa)**	**σ_z (MPa)**	**Angle (CCW with**
4+669	10.59	8.65	9.84	98º

3.3.4 2D model setup and input data

For the analysis of critical tunnel section 4+669m, the 2D box model of the tunnel having a width more than five times its excavation is constructed with boundaries restrained in both directions. The in-situ stress values are taken from the valley model, as shown in Table 6. The disturbance factor (D) has been taken as zero since it is a TBM tunnel (Hoek, 2007). The average rock mass parameters value set for analysis of chainage 4+669m is shown below in Table 6.

Table 6: The average rock mass parameter value used for the analysis of chainage 4+669m

Chainage (m)	**Density (MN/m^3)**	**Poisson's ratio**	**Ei (MPa)**	**σ_{ci} (MPa)**	**m i**	**GSI**	**σ_1 (MPa)**	**σ_3 (MPa)**	**σ_z (MPa)**
4+669	0.027	0.31	19270	34.34	7	11	10.59	8.65	9.84

Elastic analysis

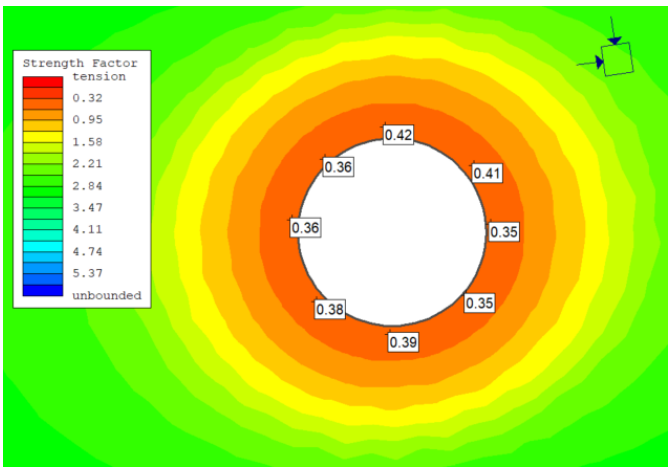

Figure 9: Strength Factor before installation of support

It is clear that the strength of the material around the tunnel's periphery, before adding support, is not strong enough. The strength factor value is less than one around the tunnel periphery as shown by the Figure 9. This means we have to investigate the possibility of material failure using plastic analysis. So, further plastic analysis is carried out.

Plastic analysis

The maximum closure (u_{max}) of the tunnel is 350mm, which occurs on the right periphery of the tunnel, and this is about 5.45% of the tunnel diameter. The plastic zone radius (R_{pl}) is 12.4m measured from center of the tunnel to the far yielded point, which is located 177.2° clockwise from the horizontal direction as shown in Figure 10.

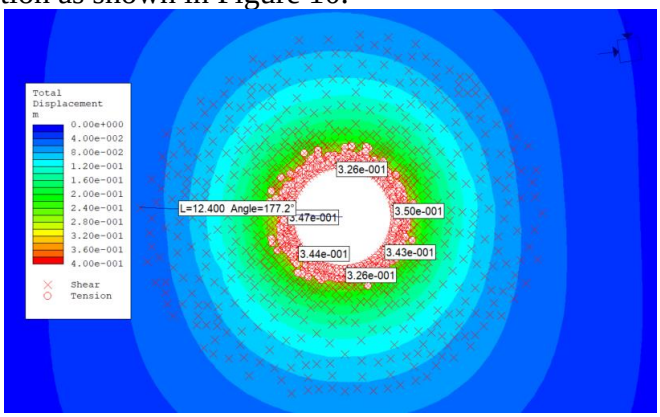

Figure 10: Total displacement and radius of plastic zone

Calculation:

- The unsupported section (X) lies almost 13m behind the tunnel face, i.e., close to the tail shield.
- Distance from tunnel face/tunnel radius = 4.06 m
- Plastic zone radius/ tunnel radius=3.875 m
- Closure/ maximum closure =0.82 [Refer to Figure 11]
- Closure = 287 mm

So, the deformation of 287 mm will occur before the support installation.

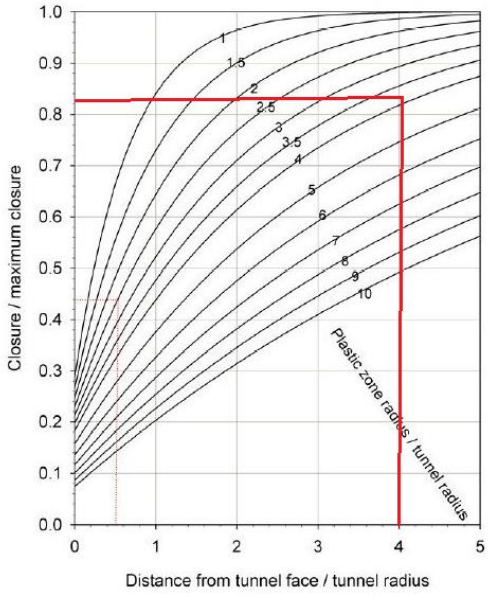

Figure 11: Improved LDP (Vlachopoulos & Diederichs, 2009)

The modeling is divided into ten stages. In the initial stage, the uniformly distributed load is applied to the tunnel periphery, balancing the effect of in-situ stress. The stage factor value is gradually reduced from 1 to 0 as we move from stage 1 to stage 10. At stage 10, maximum deformation will occur because, at this stage, internal pressure is removed, simulating the reduction of support due to the advance of the tunnel face. The relaxation stage will have deformation of about 287mm; after this stage, support will be applied.
Before the application of support, deformation of 287 mm will occur, which is far more than the void space between the shield and cutter head, even when maximum overcutting is done.

3.3.5 3D model setup and input data

RS3 software has been used for 3-dimensional analysis. RS3 is a 3D program for the analysis of geotechnical structures for civil and mining applications. RS3 is a general-purpose finite element analysis program for underground excavations, tunnel and support design, surface excavation, foundation design, embankments, consolidation, groundwater seepage, and more (Rocscience, 2023).
For the analysis of critical tunnel section 4+669m, the 3D box model having a length of 16.8m is made with a ten times expansion factor in width and height axis as shown in Figure 12The rock mass is modeled as elastic, perfectly plastic, with the generalized Hoek and Brown failure criterion. A tunnel support concrete segment of 300mm with reinforcement is designed as an elastic material.

Table 7: Model Setup in RS3

Model Setup	**RS3**
Analysis Type	Uncoupled
Solver Type	Automatic
Convergence Type	Absolute Force and Energy
Field Stress Type	Constant
Failure Criterion	Generalized Hoek and Brown
Mesh Type	4 Nodded Tetrahedron

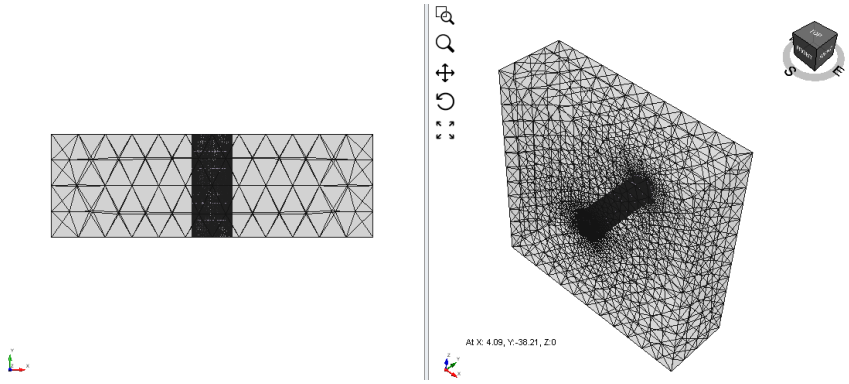

Figure 12: Model geometry for 3-dimensional analysis

The modeling is done in six stages for a 16.8m length of tunnel and the details of each stage are shown in Table .

Table 8. Stage Details

Stage	Excavation Length	Support
1	2.8 m	-
2	2.8 m	-
3	2.8 m	-
4	2.8 m	-
5	2.8 m	M50 Concrete Lining is applied in the first 2.8m excavated length
6	2.8 m	M50 Concrete Lining is applied in the next 2.8m excavated length

During the excavation of each new stage of length 2.8m, the successive reduction of deformation modulus of rock mass by half is done to incorporate the effect of decreasing support provided by the tunnel face as it moves away from particular section.

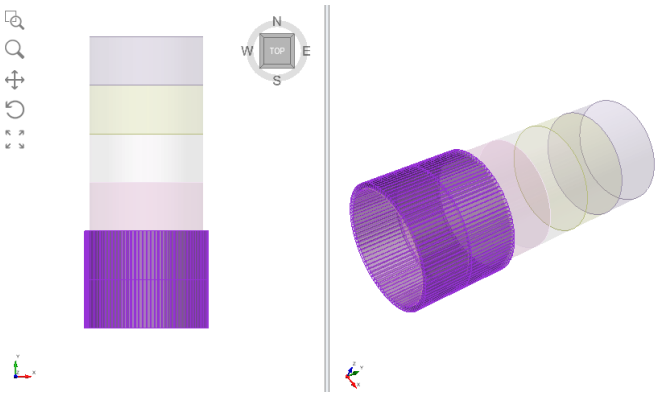

Figure 13: Top view (left) and 3d view (right) of the tunnel at the sixth stage

Elastic analysis

Initially, elastic analysis is performed considering the material properties and in-situ stress conditions as tabulated in Table 6. It is seen that the strength of the material around the tunnel's periphery before adding support is not strong enough. The strength factor value is less than one around the tunnel periphery in the longitudinal direction, as shown in Figure 14 and Figure 15. So, further plastic analysis is carried out.

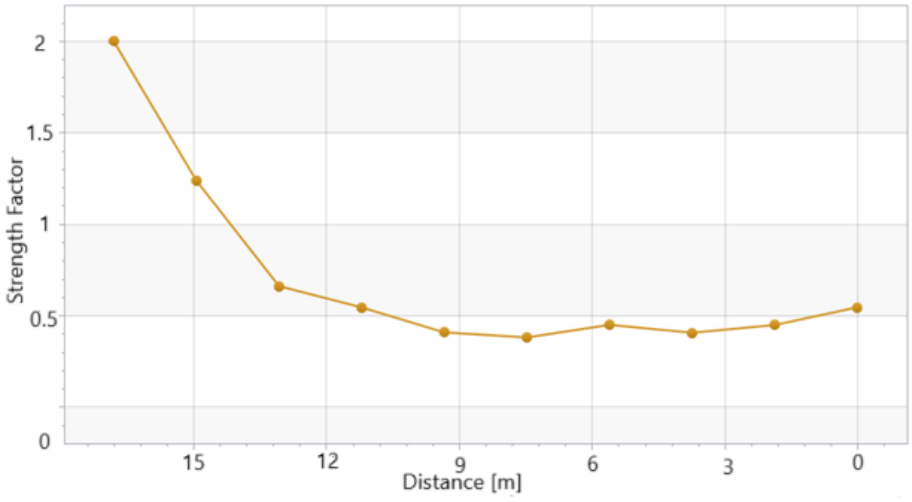

Figure 14: Strength factor along length axis at stage six

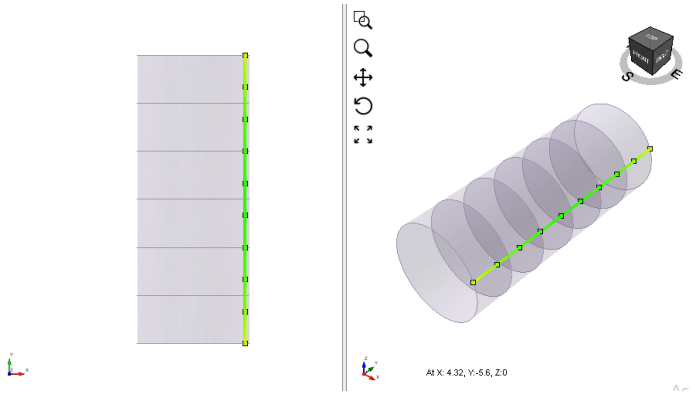

Figure 15: Line query along tunnel length axis, top view (left), and 3d-view (right)

Plastic analysis

The material starts yielding behind a 1.4m distance from the face, as shown in Figure 16. The plastic zone radius (R_{pl}) is 6.8m, measured from the center of the tunnel to the far yielded point. The deformation is an increasing trend as we go further behind the face, as shown in Figure 17. It is obvious because of the decreasing face effect as we move further behind the face. The maximum deformation of 180mm occurs at 10 m behind the face. Before the application of support, deformation of 180 mm will take place in the rear shield, which is more than the void space between the shield and cutter head, even when maximum overcutting is done.

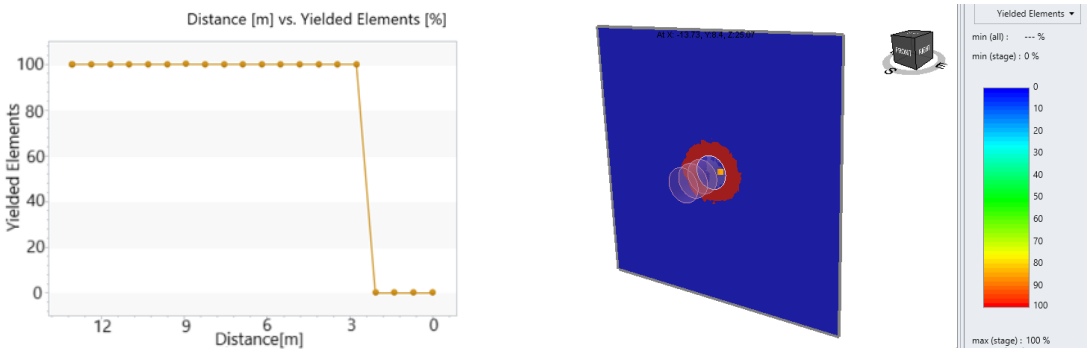

Figure 16: Yielded Element along length axis (left) and contour plane at 10m behind face (right)

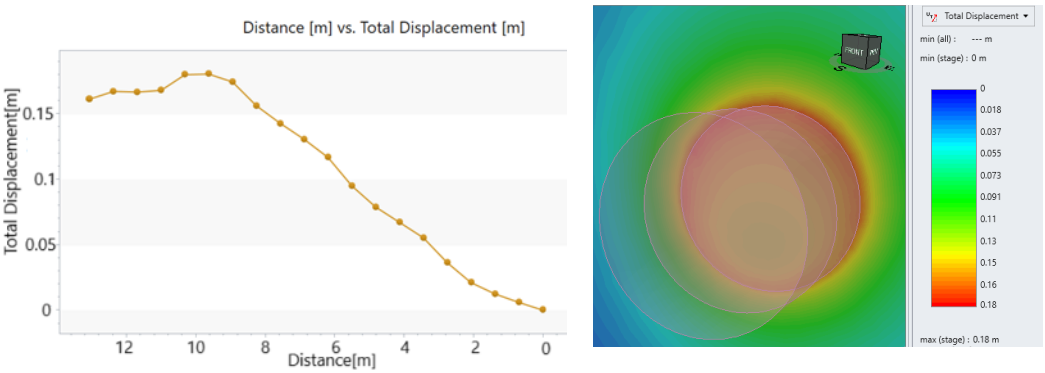

Figure 17: Deformation along the length axis ((left) and contour plane for deformation behind 10m from the face (right)

3.4 Evaluation of TBM jamming

Mainly two factors are considered for evaluation on TBM Jamming, as pointed out below:

i. Deformation on unsupported rock mass is computed, and if this deformation value is less than the void between TBM and rock mass, TBM can advance easily.

ii. If the deformation is more than the void between TBM and rock mass, there will be contact between the surrounding rock mass and the shield, and the rock pressure is exerted on the shield. In this case, the required thrust force Fr to overcome shield skin friction can be calculated by integrating the ground pressure over the shield surface. If Fr is less than the installed thrust capacity, there will be the risk of TBM jamming.

From Section 3, at chainage 4+669m there is possible squeezing that may cause jamming of TBM. So, the required thrust force F_r is estimated based on the nomogram proposed for Double Shield TBM (Romani & Anagnostou, 2010). The required thrust force F_r depends on the material constants of the ground (Deformation modulus E, Poisson's ratio ν, uniaxial compressive strength f_c, angle of internal friction φ and dilatancy angle Ψ), the initial stress σ_o, the characteristics of the TBM (tunnel radius R, radial gap size △R, shield length L and shield stiffness K_s), the skin friction coefficient μ and the stiffness of the lining K_l (Ramoni & Anagnostou, 2010).

Table 8: Calculation for the required thrust force for double shield TBM to overcome shield skin friction in squeezing ground (Ramoni & Anagnostou, 2010)

S.N.	Ground	Symbol	Unit	Ch 4+669 m	Remarks
1	Deformation Modulus	E	MPa	620	
2	Uniaxial compressive strength	f_c	MPa	1.56	
3	Angle of internal friction	φ	°	20	
4	Dilatancy angle	Ψ	°	1	(P.A. Vermeer, 1984)
5	Unit weight	γ	KN/m^3	27	
	Initial stress				
6	Overburden	H	m	350	
7	Initial stress	σ_o	MPa	9.45	$\sigma_o = \gamma.H$
	TBM				
8	Boring radius	R	m	3.2	
9	Radial Gap Size, forward shield	$\triangle R_f$	cm	10.5	
10	Radial Gap Size, rear shield	$\triangle R_r$	cm	15.5	
11	Length of forward shield	L_f	m	5.2	
12	Length of rear shield	L_r	m	7.8	$L_r = 1.5 x L_f$
13	Length of shield	L	m	13	
14	Normalized Shield length	L/R		4.062	
15	Young's Modulus	E_s	MPa	210000	
16	Thickness Shield	d_s	cm	12	
17	Stiffness of Shield	K_s	MPa/m	2460	$K_s = E_s . d_s / R^2$

S.N.	Ground	Symbol	Unit	Ch 4+669 m	Remarks
	Dimensionless products				
18	$(E\triangle R_f)/(\sigma_o R)$			2.15	
19	$(E\triangle R_r)/(\sigma_o R)$			3.17	
20	f_c/σ_o			0.16	
	Thrust force requirement				
	Forward Shield				
21	Normalized required thrust@3.5			0.058	Refer to Figure 18 (left)
22	Normalized required thrust@5.0			0.07	Refer to Figure 18 (right)
23	Normalized required thrust@4.062 [by interpolation]			0.06	
24	Required thrust force	$F_{r,f}$	MN	46.313	
	Rear Shield				
25	Normalized required thrust@3.5			0.048	Refer to Figure **19** (left)
26	Normalized required thrust@5.0			0.06	Refer to Figure **19** (right)
27	Normalized required thrust @ 4.062 [by interpolation]			0.05	
28	Required thrust force	$F_{r,r}$	MN	38.903	
29	Total required thrust force	F_r	MN	85.216	

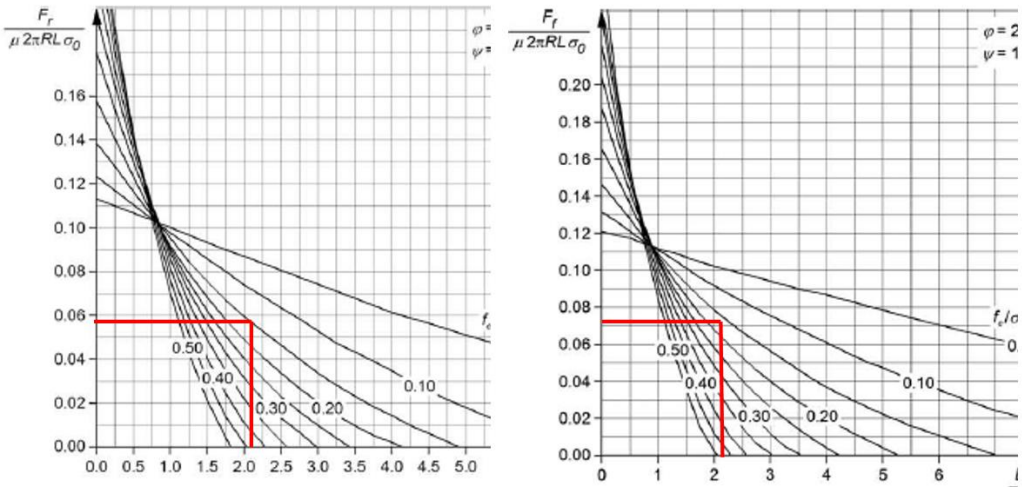

Figure 18: Nomograms for the front shield of a double-shielded TBM normalized shield length 3.5(left) and 5.0 (right)

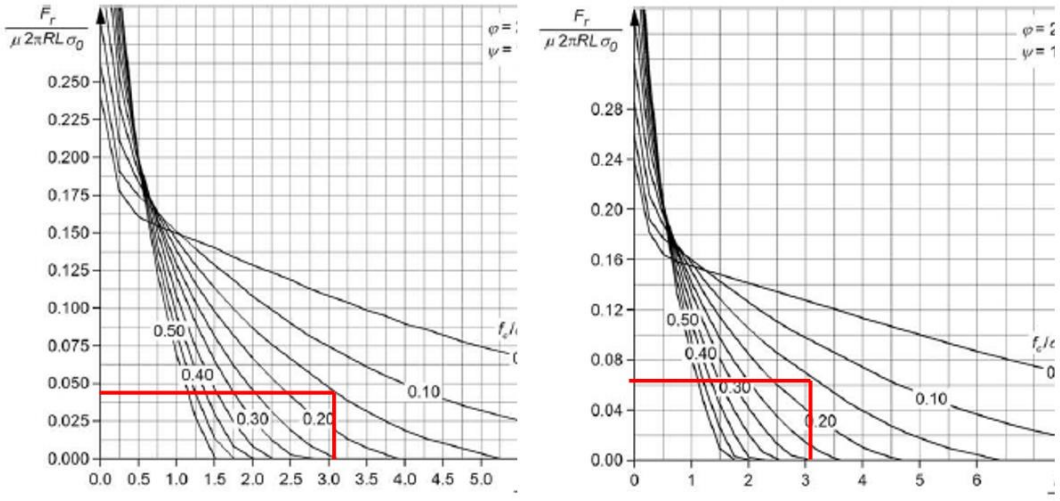

Figure 19: Nomograms for the rear shield of a double-shielded TBM normalized shield length 3.5(left) and 5.0 (right)

The double shield TBM used in SMDMP has a maximum thrust capacity of 47,124 KN provided by 17 jacks. From Table 8, the required thrust capacity is 85,000 KN even when considering the maximum overcutting possible by the machine, i.e., 10.5cm for the forward shield and 15.5cm for the rear shield. Therefore, the TBM thrust capacity is less than the required thrust capacity Fr to overcome shield skin friction. The TBM also got stuck due to squeezing at chainage 4+669.

4. Conclusion

This paper aims to highlight the importance of overcutting and thrust capacity of TBM machines in squeezing ground conditions, along with prior identification of rock mass properties at respective sections.

During the critical section, between the two thrust zones, particularly located close to each other, probe hole drilling is the most important method to foresee the actual rock mass condition along with Horizontal Seismic Profiling. The selection of overcutting and thrust capacity of double shield TBM is the necessary factor to overcome shield skin friction. In our case, the deformation outcomes from 2-D and 3-D analysis, 287mm and 180mm, respectively, are greater than the overcutting capacity of 140mm at the critical section. Therefore, the deformation at the critical section should be considered before manufacturing the double-shield TBM. The thrust capacity used for overcoming skin friction plays a decisive role in generating the necessary force to move the machine forward. Thus, optimizing the thrust capacity is crucial, considering the critical section where immense deformation may occur.

Acknowledgment

The authors are thankful to the SMDMP project for providing the information related to the project.

Conflict of interest

The authors declare no conflict of interest. This research paper has been written solely for educational purposes and is not intended to be used as a supporting document for any legal, commercial, or other issues. The views and findings presented are for academic and research purposes only.

References

[1] KC, D., Gautam, K., H., Kadel, S., & Hu, L. (2022). Challenges in Tunneling in the Himalayas: A Survey of Several Prominent Excavation Projects in the Himalayan Mountain Range of South Asia. *Geotechnics*, *2*(4), 802–824. https://doi.org/10.3390/geotechnics2040039

[2] Singh, B. P., & Goal, R. K. (2006). *Tunnelling in Weak Rocks*. https://api.semanticscholar.org/CorpusID:126838427

[3] SMDMP. (2020). Geotechnical Baseline Report of Sunkoshi Marin Diversion Multipurpose Project. [Hardcopy]. Accessed in March 2023.

[4] Bohara, B., Bhattarai, T. R., Shilpakar, P., & Katuwal, T. B. (2023). *IOE Graduate Conference Construction Challenges Encountered During Shield TBM Tunneling in Sunkoshi Marin Diversion Multipurpose Project, Sindhuli, Nepal*. https://conference.ioe.edu.np/publications/ioegc14/IOEGC-14-005-A2-1-207.pdf

[5] Ramoni, M., & Anagnostou, G. (2010). Thrust force requirements for TBMs in squeezing ground. *Tunnelling and Underground Space Technology*, *25*(4), 433–455. https://doi.org/10.1016/j.tust.2010.02.008

[6] Hoek, E. (2007). Practical Rock Engineering. https://www.rocscience.com/assets/resources/learning/hoek/Practical-Rock-Engineering-Full-Text.pdf

[7] Panthi, K. K. (2012). Evaluation of rock bursting phenomena in a tunnel in the Himalayas. *Bulletin of Engineering Geology and the Environment*, *71*(4), 761–769. https://doi.org/10.1007/s10064-012-0444-5

[8] Vlachopoulos, N., & Diederichs, M. S. (2009). Improved longitudinal displacement profiles for convergence confinement analysis of deep tunnels. *Rock Mechanics and Rock Engineering*, *42*(2), 131–146. https://doi.org/10.1007/s00603-009-0176-4

[9] *Rocscience*. (2023). 2D and 3D Geotechnical Software. Retrieved April 2023. https://www.rocscience.com/